

Evidence for an ionic model of 3d impurities in metals

John A. Gardner

Department of Physics, Oregon State University, Corvallis, Oregon 97331

(Received 2 June 1975)

The orbital susceptibility of Co impurities in several metals is shown to be consistent with an ionic model suggested by Hirst which is generalized to include strong lifetime broadening of the many-body ionic energy levels by k - d interaction. Kondo and both intra- and interconfiguration fluctuations are included. In CuCo and AuCo at low temperature the 3d ionic ground state is a T_{1g} orbital triplet which is broadened to about 0.1 and 0.02 eV, respectively. In liquid CuCo the ionic state is apparently an unsplit 4F orbital. In nonmagnetic Co systems ionic linewidths may be several eV, but only a few distinct ionic orbitals are coupled into the ground state. In AlCo , the ionic state is about 2.5 eV wide and is a superposition of either a 4F and 4P (intraconfiguration fluctuation), or a 4F and 5D (interconfigurational fluctuation). These considerations strongly indicate that localized spin fluctuation and other band-type models are not appropriate for 3d impurities.

I. INTRODUCTION

When a transition-metal impurity is dissolved into a nonmagnetic metal, one observes a wide variety of magnetic properties, ranging from strongly magnetic (AuFe , CuMn , etc.) to nonmagnetic (CuNi , AlV). Theorists have proposed an equally wide variety of possible models for the impurity state, but most can be grouped into two categories. One is the "magnetic" group which picture the impurity as a reasonably well-defined ionic configuration whose Zeeman levels are broadened and coupled by conduction-electron interaction.^{1,2} The second category includes the Friedel virtual-bound-state model,³ the nonmagnetic Anderson model,⁴ and the various localized-spin-fluctuation⁵ models which assume a zero-order bandlike picture for the impurity d electrons with fluctuating spin and orbital moments caused by residual ionic exchange interactions. Both approaches are physically equivalent when properly formulated. However, the theoretical approximations (perturbation treatment, Hartree-Fock, random-phase approximation, etc.), which are normally used make these models proper only when the intraionic interactions are strong (magnetic group) or weak (nonmagnetic group) with respect to ion-conduction-electron interaction. This distinction may be meaningless for a nondegenerate model but is important for real orbitally degenerate impurities.⁶ Unfortunately, it has proven difficult to tell which group if either, describes real impurities.

The ionic structure of transitional impurities has been discussed extensively by Hirst⁷ for impurities with ground ionic levels which are not strongly perturbed by interaction with conduction electrons. This weak-interaction approximation is known to be valid for many rare-earth impurities and compounds but is not obviously applicable for transi-

tion-metal impurities. Except for a few "bottlenecked" impurity systems, EPR lines are too broad to be useful in identifying ionic level structure. Optical measurements are very difficult, and interpretation is ambiguous.

Since there has been little firm evidence of detailed ionic structure, the intraionic interactions usually are approximated by a greatly simplified generalization of the Anderson model.⁴ Although this simplification has made quantitative calculation of thermodynamic properties tractable in special cases,^{5,8} it may have obscured some important physical properties as well. In this paper the ionic structure of the particularly interesting Co impurity will be discussed in detail, and it is shown that proper consideration of orbital and crystal-field splitting resolves several puzzling experimental observations. These considerations indicate that the local d state of Co impurities is a superposition of a small number of many-body ionic orbital levels. The implication is that the localized-spin-fluctuation group of theoretical models which are basically interacting one-electron approximations does not provide a useful picture of the localized impurity d state of transition impurities. A model which assumes a well-defined many-body ionic orbital ground state such as a generalized Kondo model seems to be a much more realistic approximation.

II. Co IONIC LEVEL STRUCTURE

Cobalt is a particularly favorable impurity for studying orbital effects, since it is known to display large orbital paramagnetism when dissolved into most normal cubic metals. This is indicated by large positive Co Knight shifts observed in such systems as AuCo ,⁹ CuCo ,¹⁰ and liquid $\text{Cu}_x\text{Al}_{1-x}\text{Co}$.¹¹

As discussed by Hirst,⁷ Co impurities in the ground state should have configuration $(3d)^7k^2$,

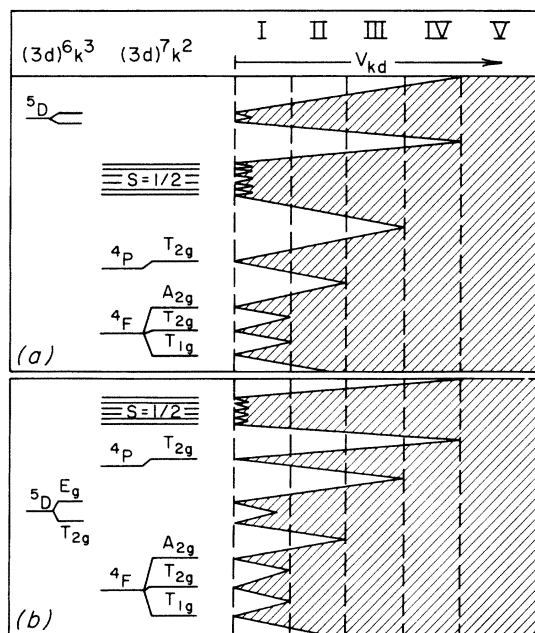


FIG. 1. Schematic diagram of lower-lying ionic energy levels of Co. The metal conduction band includes the valence (k) impurity electrons and is assumed to be in its ground state, so ionic labels refer only to $3d$ core. Broadening and overlap due to k - d mixing interaction V_{kd} are shown on right-hand side.

where k denotes the predominantly s - p symmetry (conduction) electrons. The ionic energy levels for this and the neighboring $(3d)^6k^3$ configuration are shown in Fig. 1. This diagram shows two extreme possibilities where the low-lying states of the two configurations are (a) very well separated or (b) very close in energy. Other configurations and the band of excited many-body conduction electron states attached to each ionic level are omitted for simplicity.

In the level diagrams of Fig. 1 spin-orbit coupling is ignored and an intermediate cubic crystal-field is assumed. These approximations are qualitatively but probably not quantitatively valid for all cases we consider. The T_{1g} crystal-field ground state and its 4F parent level both have large orbital moments in a magnetic field, in agreement with experimental observations.

When a k - d interaction V_{kd} is allowed, ionic energy levels in a configuration having n $3d$ electrons are coupled to numerous levels in configurations with $n \pm 1$ $3d$ electrons in first order, n and $n \pm 2$ $3d$ electrons in second order, etc. When V_{kd} is very small, the Zeeman levels of the lowest-lying ionic orbital are coupled and lifetime broadened by even order (Kondo-type) interactions, but higher-lying distinct orbitals are not significantly coupled into the ground state levels. When V_{kd} is larger

these higher-lying orbitals can become strongly coupled to the original ground state orbitals. This happens when the lifetime broadening becomes comparable to the level separations. In Fig. 1, the ionic level widths are indicated schematically versus V_{kd} . The region in which the lowest crystal field orbital overlaps no other ionic level is labeled I in Fig. 1. Beyond I the "ground state" becomes a superposition of several orbital levels, and four important regions are labeled. II is similar to I except that crystal-field splitting is washed out by V_{kd} . In III the ionic linewidths are large enough that crystal-field splitting is negligible, and only one otherwise distinct ionic orbital overlaps strongly with the low-lying 4F ionic level. The two possibilities shown correspond to an intraconfigurational fluctuation (low-lying 4P state of same configuration) or interconfigurational fluctuation [low-lying 5D state of $(3d)^6k^3$ configuration] of the impurity ion. If the level separations are small, regions II and III cannot be separated as shown. In IV, V_{kd} is so large that many otherwise distinct ionic levels contribute to the ground state, but considerable many-body ionic character still remains. There are of course numerous other orbital superpositions which can occur besides the ones shown. V indicates the region in which essentially all many-body $3d$ orbitals contribute to the ground level and a one-electron description becomes preferable.

The energy-level diagrams shown in Fig. 1 may be considered a generalization of the orbitally degenerate Anderson model in which considerably more complicated intraionic interactions are included. Previously only a spin-spin repulsion energy \bar{J} has been included^{4,6,12}; in this approximation all levels of the same spin in any given configuration are degenerate. For this special case, regions I and II merge into III(a) and the quartet-doublet spin splitting in $(3d)^7k^2$ is $3\bar{J}$. Other models may be classified approximately in terms of Fig. 1 also. The usual Kondo¹ model also neglects crystal field and purely orbital ionic splitting and would apply to an ionic state in region III(a). The s - d interaction does not completely describe the interaction between conduction electrons and the ionic Zeeman levels if the ground state is orbitally degenerate but can be generalized to this case.⁷ It can also be generalized to regions I and II but cannot describe transitions between regions. The Friedel-Anderson^{3,4} nonmagnetic virtual bound state model is valid in region V. The spin-split magnetic version of that model is included in region IV but is, in principle, similar to III(b) since it includes high-spin many-body orbitals from all configurations in the ground state. Enhanced susceptibility models such as the localized-spin-fluctuation⁵ and Anderson-model random-phase approx-

imation⁸ describe the transition from V to IV.

III. Co MAGNETIC PROPERTIES

Co impurities are usually classified as nonmagnetic or weakly magnetic when compared to Cr, Mn, and Fe. The latter three, for example, display Curie-like susceptibilities except at very low temperatures, when they are dissolved in noble metals. The impurity susceptibility of CuCo, however, is only weakly temperature dependent, decreasing from approximately 2.3×10^{-3} cm³/mole at¹³ 4 K to 1.2×10^{-3} cm³/mole at the melting point.¹⁴ In Au, the Co susceptibility is larger at low temperature and more strongly temperature dependent.¹⁵

Recently, Ritter, Bremer, and Gardner¹¹ measured the Co Knight shift in liquid $Cu_xAl_{1-x}Co$ alloys in which the Co susceptibility ranges from about 10^{-4} cm³/mole in AlCo up to 1.2×10^{-3} cm³/mole in CuCo.¹⁶ They found a linear relationship between the Co Knight shift κ and susceptibility χ over a wide host composition and temperature range. Representative data are shown in Fig. 2, and it is seen that only the point corresponding to CuCo falls significantly off the solid line. κ is related to the Co spin and orbital susceptibility by

$$\kappa = \kappa_0 + \alpha \chi_{orb} + \beta \chi_{spin}, \quad (1)$$

where κ_0 is the (approximately constant) Fermi contact term. α is the orbital hyperfine coupling

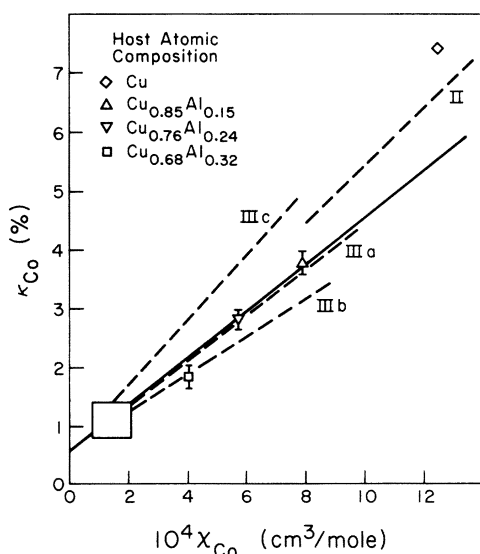


FIG. 2. Co Knight shift vs Co susceptibility in liquid $Cu_xAl_{1-x}Co$. Data are taken from Ref. 11. The solid line is an extrapolation of the best-fit straight line to data in the boxed region. These data are taken for host alloys with less than 55% Cu and are shown on expanded figures in Ref. 11. The dashed lines are given by the broadened ionic model for the labeled orbital overlap regions.

constant which should be approximately 120 mole/cm³,¹⁷ and β is the core (including conduction electron) polarization coupling constant which is typically -10 mole/cm³ for 3d impurities.¹⁸ Figure 2 indicates that the second term in Eq. (1) is dominant and that for $\chi < 8 \times 10^{-4}$ cm³/mole the orbital and spin susceptibility must increase roughly proportionally versus temperature and host composition.

The linearity of Fig. 2 for nonmagnetic impurities is consistent with an impurity state in region V or an intermediate "spin-fluctuation" region similar to IV(a) of Fig. 1 in which all orbitals of a given configuration are either completely excluded or equally represented in the ground state. This is the situation represented by the Anderson model if $\bar{J} = 0$. It is not difficult to show that in this case the orbital moment is always twice the spin moment. The susceptibility depends on the bandwidth, but the spin and orbital susceptibility are everywhere proportional.

This interpretation of their data led Ritter *et al.*¹¹ to three serious inconsistencies. First, using the above hyperfine coupling constants and Eq. (1), the slope $\Delta\kappa/\Delta\chi$ in regions IV(a) and V should be 77 mole/cm³, well above the experimental value of 40 mole/cm³. Secondly, these data fix an upper limit of considerably less than 0.3 eV for the Hund's exchange energy \bar{J} of nonmagnetic Co impurities. This is several times smaller than a similar analysis indicates for \bar{J} of Mn.¹⁹ If \bar{J} is less than 0.3 eV all energy levels of the $(3d)^7k^2$ configuration must lie within a range of 1 eV or less, more than an order of magnitude smaller than in a free ion. Third and most significant, the Knight shift of Co in liquid CuCo lies well above the extrapolated solid line in Fig. 2 whereas the model requires it to lie on or below the line. κ should lie on the line if the impurity level width in CuCo remains much greater than \bar{J} . Otherwise, the ratio of orbital to spin moment must decrease, $d\kappa/d\chi$ must also decrease as a consequence of Eq. (1), and κ must fall below the line. Ritter *et al.* discussed this discrepancy in terms of the generalized Anderson random-phase-approximation susceptibility,⁸ but it is a general feature of any model in this transition region. A final puzzling feature is that the Co Knight shift decreases from 7.4% in liquid CuCo to 5.2% at 4 K,¹⁰ although the susceptibility increases by almost a factor of 2.

We propose that the discrepancies arise because the Co ionic state in liquid Al and Al_xCu_{1-x} hosts is not in regions IV or V but rather in region III where ionic level widths and spacings are both of order a few eV. As shown below, this assumption is also consistent with the observed constant χ_{orb}/χ_{spin} ratio. In CuCo and AuCo the ionic level widths are much smaller, and a region

I description is proper at low temperature. In liquid copper the combined broadening effects of V_{kd} and temperature apparently wash out instantaneous crystal-field splittings such that a region II state becomes appropriate. In Sec. IV we compute the static magnetic properties of Co impurities in each of the regions shown in Fig. 1 and show that experimental data is in excellent agreement with these suppositions.

IV. MAGNETIC PROPERTIES OF BROADENED IONIC STATES

Even under the simplest possible assumptions, it is clearly a formidable problem to compute precise properties of an ionic model like that pictured in Fig. 1. Nevertheless a semiquantitative characterization of static magnetic properties can be derived by simple intuitive reasoning. Fortunately, this is sufficient to provide a surprisingly detailed picture of the ionic structure.

The magnetic susceptibility of a region-I ion will exhibit normal Curie-like susceptibility only when $T \gg T_K$, where kT_K is the ionic linewidth or equivalently the average off-diagonal matrix element splitting otherwise degenerate Zeeman levels. At low temperatures the susceptibility approaches a constant. A reasonable and common approximation is to assume a $(T + T_K)^{-1}$ form for the (zero-field) susceptibility. As an example, when $T + T_K$ is much smaller than the crystalline-field splitting the susceptibility of a region-I Co ion would be

$$\chi_{\text{spin}} = \mu_B^2 g_s^2 S(S+1) / 3k_B(T + T_K), \quad (2)$$

$$\chi_{\text{orb}} = \mu_B^2 g_L^2 \tilde{L}(\tilde{L}+1) / 3k_B(T + T_K). \quad (3)$$

Here $g_s = 2$ and $S = \frac{3}{2}$. For the T_{1g} triplet, $g_L = -\frac{3}{2}$, and $\tilde{L} = 1$. When $T + T_K$ is greater than the crystalline-field splitting, the susceptibility is the same as if the 4F level were unsplit (i. e., a region-II ionic state) by the Van Vleck theorem.²⁰ In this case, χ_{spin} is the same as above but $g_L = 1$, and $\tilde{L} = L = 3$. When the ionic ground state is a superposition of distinct orbital levels which are not coupled by the magnetic field such as in regions III to IV, the total susceptibility is an appropriately weighted average.

In Table I, $\langle g_s^2 S(S+1) \rangle$, $\langle g_L^2 L(L+1) \rangle$, and $\chi_{\text{orb}} / \chi_{\text{spin}}$ are tabulated for regions I, II, III(a), III(b), IV(a), and V shown in Fig. 1. Also included is region III(c) which is not shown in Fig. 1. This is the overlap region similar to III(b) when the low-lying ionic excited state is the 3F orbital belonging to configuration $(3d)^9 k^1$. We assume that T_K is the same for all the distinct orbital levels which contribute to the susceptibility and neglect all other contributions to the impurity susceptibility. Van Vleck orbital paramagnetism²⁰ is probably the only significant neglected quantity, and it should be

TABLE I. Spin and orbital contributions to the Co susceptibility. The regions refer to different superpositions of orbitals illustrated in Fig. 1. Region III(c) is explained in text.

	Regions						
	I	II	III(a)	III(b)	III(c)	IV(a)	V
$\langle g_s^2 S(S+1) \rangle$	15	15	15	19.25	12	7	7.5
$\langle g_L^2 \tilde{L}(\tilde{L}+1) \rangle$	4.5	12	9	9.17	12	14	15
$\chi_{\text{orb}} / \chi_{\text{spin}}$	0.3	0.8	0.6	0.476	1.0	2.0	2.0

small except in region I when $T + T_K$ is of order the crystal-field level spacing.

Since the experimental data of interest are κ and χ , it is convenient to consider the ratio

$$\frac{\kappa - \kappa_0}{\chi} = \alpha \left(1 + \frac{\chi_{\text{spin}}}{\chi_{\text{orb}}} \right)^{-1} + \beta \left(1 + \frac{\chi_{\text{orb}}}{\chi_{\text{spin}}} \right)^{-1}. \quad (4)$$

Using the α and β above, this ratio is shown in Fig. 3 versus $T + T_K$ and the corresponding susceptibility (upper scale). The dividing lines are chosen to place the experimental data into what appear to be the appropriate regions. These divisions are not unreasonable but in the absence of information about ionic structure cannot be further supported. In addition to the experimental data for liquid $\text{Cu}_x\text{Al}_{1-x}\text{Co}$ discussed above, liquid SnCO (Refs. 21 and 22) and low-temperature CuCo (Refs. 10 and 13) and AuCo (Refs. 9 and 15) data are also shown.

The error bars on the experimental data in Fig. 3 are due to uncertainty in κ_0 and χ . There is also an uncertainty of perhaps 25% in the computed ratio because of uncertainty in α . The uncertainty in β should contribute little error by comparison. It is unlikely that the coupling constant depends strongly on the ionic region, so any errors in α would cause an approximately uniform shift of all the computed values. Within these limitations it is clear that the experimental data are very well described by this broadened ionic model provided the "nonmagnetic" Co impurity state is in region III(a) or III(b). The intraconfiguration fluctuation model of Fig. 1(a) is in better agreement with the experimental results in region III, but in the interconfiguration fluctuation model of Fig. 1(b) better describes the transitions between regions II and III. Either are in good semiquantitative agreement with experiment which is all that can be expected from these simple considerations. The fit to experiment is also indicated for the data shown in Fig. 2 where labeled dashed lines are shown for regions II and III(a), III(b), and III(c). The good fit of the solid CuCo results to region I properties indicates that our neglect of Van Vleck paramag-

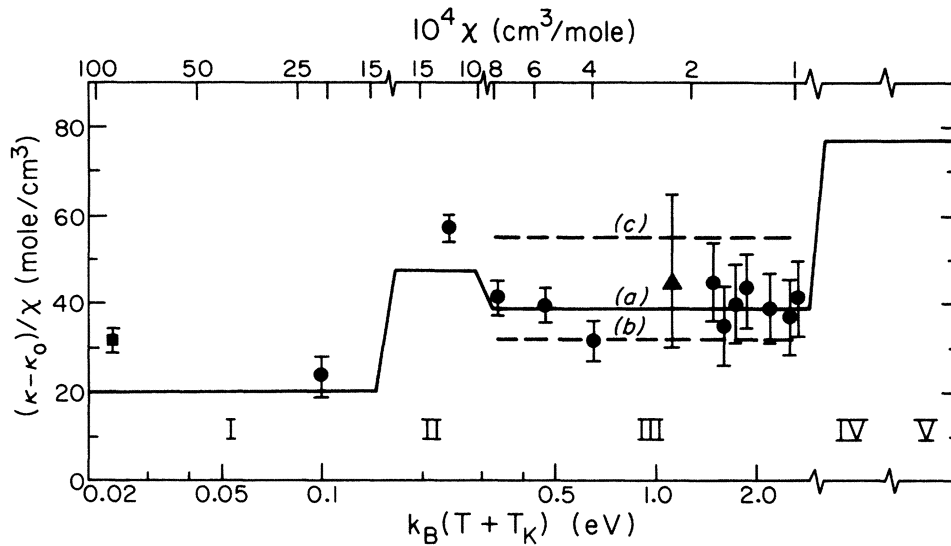


FIG. 3. Ratio of Co Knight shift to Co susceptibility vs total level broadening energy $k_B(T + T_K)$. Division by region is arbitrarily chosen to place data into appropriate probable orbital overlap region. Co susceptibility obtained from Table I for the (a) regions is shown on upper scale. Circles are data for solid low temperature CuCo (region I, Refs. 10, and 13); liquid CuCo (region II, Ref. 11); and liquid $\text{Cu}_x\text{Al}_{1-x}\text{Co}$ (region III, Ref. 11). Square is for low-temperature AuCo (Refs. 9 and 15). Triangle is for liquid SnCo (Refs. 21 and 22).

netism is valid and implies that the total crystal-field level spacing of 4F -derived levels is at least 4 or 5 times the level width, or about $\frac{1}{2}$ eV. Since the liquid CuCo impurity state is in region II, the average crystal-field splitting is much smaller in the liquid. This is hardly surprising since the "crystal-field" perturbation in the liquid state differs significantly from the low-temperature cubic crystalline field. The position of the crossover between region II and III in Fig. 3 yields an estimate of about 0.3 eV for the separation between the 4F and 4P or 4F and 5D orbitals.

The above interpretation of the low- and high-temperature CuCo data is internally consistent, since the same value $k_B T_K \approx 0.1$ eV is required in each case to fit the magnitude of χ . In addition, the slope of χ in the liquid state is well fit by a $(T + \Theta)^{-1}$ dependence, where $\Theta = T_K \approx 1400$ K. In AuCo at low temperature $\Theta \approx 200$ K,¹⁵ also in good agreement with the T_K of about 300 K found above. We note however that our neglect of spin-orbit coupling is not completely valid if the ionic linewidth is smaller than 0.1 eV.

V. CONCLUSIONS

The general picture of the Co impurity state that emerges from these considerations can be summarized by reference to the ionic-level diagrams of Fig. 1. The total crystal-field splitting of the 4F ground-state parent level is apparently about the same as in similar insulating materials, of order 1 eV. When the metal is liquified, the

"crystal fields" evidently become negligible since the susceptibility of liquid CuCo indicates an unsplit 4F ionic ground state and the same level width found in the solid. As Al is added to the liquid metal the ionic linewidth broadens and overlaps the higher-lying 4P or 5D orbital. In liquid AlCo the ionic linewidth is 2.5 eV. This broadened ionic picture is semiquantitatively successful in relating the large positive Co Knight shifts observed in low-temperature Au and Cu and in liquid Cu, Al, Sn, and $\text{Cu}_x\text{Al}_{1-x}$ hosts to the Co susceptibility. These data are not in good agreement with either the localized spin fluctuation or enhanced virtual state models nor with a simple Kondo model which does not properly account for ionic structure. Liquid alloy data have been fit by Peters and Flynn²³ to an excited spin-only ionic model, but this model neglects observed orbital susceptibilities and does not apply at low temperature.

Similar broadened ionic diagrams can be drawn for other transitional impurities, and experimental information on the hyperfine fields and susceptibility of 3d elements in normal metals are consistent with this picture. Except for the Co results discussed above, data are generally not complete enough to determine a great deal about the ionic structure, or provide any strong evidence in favor of this model over most others. If one assumes an ionic picture however, it is possible to make a few deductions about the ionic level structure. For example, Hirst⁷ showed that the ground configuration of "magnetic" impurities near the center of the 3d row is $(3d)^n k^2$. Orbital contributions to non-

magnetic Mn Knight shifts²⁴ indicate an orbitally degenerate ionic level lying about 1 eV above the ground 6S level. The V Knight shift²⁵ is consistent with the expected A_2 cubic crystal-field ground state of the $(3d)^3k^2$ configuration and a crystal-field splitting about the same magnitude as found above for Co.⁶

It should be noted that extensive modification of

the ionic structure can occur through $d-d$ interactions, and these are explicitly ignored in the model presented here. Consequently, this very simple crystal-field approximation may not be applicable for impurities in more complicated materials and will certainly be improper for very concentrated alloys and pure transition metals.

¹J. Kondo, *Prog. Theor. Phys.* **32**, 37 (1964).

²Several review articles on Kondo theory appear in *Magnetism*, edited by G. Rado and H. Suhl (Academic, New York, 1973), Vol. V.

³J. Friedel, *Adv. Phys.* **3**, 446 (1954).

⁴P. W. Anderson, *Phys. Rev.* **124**, 41 (1961).

⁵D. L. Mills, M. T. Béal-Monod, and P. Lederer, in Ref. 2.

⁶L. Dworin, *Phys. Rev. Lett.* **26**, 1372 (1970).

⁷L. L. Hirst, *Phys., Kondens. Mater.* **11**, 255 (1970); *Z. Phys.* **245**, 378 (1971); *Intern. J. Magn.* **2**, 213 (1972).

⁸L. Dworin and A. Narath, *Phys. Rev. Lett.* **25**, 1287 (1970).

⁹A. Narath and D. C. Barham, *Phys. Rev. B* **7**, 2195 (1973).

¹⁰S. Wada and K. Asayama, *J. Phys. Soc. Jpn.* **30**, 1337 (1971).

¹¹A. L. Ritter, J. C. Bremer, and J. A. Gardner, *Phys. Rev. B* **10**, 3246 (1974).

¹²B. Caroli, C. Caroli, and O. R. Fredkin, *Phys. Rev.* **178**, 599 (1969).

¹³R. Tournier and A. Blandin, *Phys. Rev. Lett.* **24**,

397 (1970).

¹⁴J. A. Gardner and C. P. Flynn, *Philos. Mag.* **15**, 1233 (1967).

¹⁵E. Boucai, B. Lecoanet, J. Philon, J. L. Thoulence, and R. Tournier, *Phys. Rev. B* **3**, 3834 (1971).

¹⁶J. Bensele and J. A. Gardner, *Phys. Rev. B* **9**, 4303 (1973).

¹⁷This value is obtained from A. J. Freeman and R. E. Watson [*Magnetism*, edited by G. Rado and H. Suhl, Vol. IIA (Academic, New York, 1965)] by assuming a 10% decrease of $\langle r^{-3} \rangle$ in metals.

¹⁸A. Narath, in Ref. 2.

¹⁹W. W. Warren, Jr., R. E. Walstedt, and Y. Yafet, *Bull. Am. Phys. Soc.* **19**, 203 (1974).

²⁰J. H. Van Vleck, *The Theory of Electric and Magnetic Susceptibilities* (Oxford U.P., Oxford, 1932).

²¹R. Dupree, *Phys. Lett. A* **44**, 435 (1973).

²²S. Tamaki, *J. Phys. Soc. Jpn.* **25**, 1602 (1968).

²³J. J. Peters and C. P. Flynn, *Phys. Rev. B* **6**, 3343 (1972).

²⁴R. E. Walstedt and W. W. Warren, Jr., *Phys. Rev. Lett.* **31**, 365 (1973).

²⁵A. Narath, *Solid State Commun.* **10**, 521 (1972).